Austrian Journal of Earth Sciences | Volume 107/2 | 100 - 111 | Vienna | 2014

Lack of evidence for impact signatures in Neoproterozoic postglacial deposits from NW-Namibia

Ildikó GYOLLAI[1)2)3)], Dieter MADER[1)], Márta POLGÁRI[3)*)], Friedrich POPP[4)] & Christian KOEBERL[1)5)]

[1)] Department of Lithospheric Research, University of Vienna, Althanstrasse 14, 1090 Vienna, Austria;

[2)] Cosmic Materials Research Group, Eötvös Loránd University of Budapest (ELTE), Pázmány Péter sétány 1/A, 1117 Budapest, Hungary;

[3)] Research Center for Astronomy and Geosciences, Geobiomineralization and Astrobiological Research Group, Institute for Geology and Geochemistry, Hungarian Academy of Sciences, Budaörsi út 45, 1112 Budapest, Hungary;

[4)] Department of Geodynamics and Sedimentology, University of Vienna, Althanstrasse 14, 1090 Vienna, Austria;

[5)] Natural History Museum, Vienna, Burgring 7, 1010 Vienna, Austria;

[*)] Corresponding author, rodokrozit@gmail.com

KEYWORDS

Snowball Earth
Neoproterozoic
boundary layer
impact event

Abstract

At least two global Neoproterozoic (Cryogenian) glaciation events ("Snowball Earth") occurred 710 Ma (Sturtian) and 630 Ma (Marinoan) ago, during which the oceans were either completely frozen or at most a few small open water oases remained. Neither the cause of the onset of the glaciations, their extent and duration, nor the cause for the deglaciations, are currently fully understood.

In this study we try to follow up earlier studies by our group that indicated the presence of an extraterrestrial signature in rock units that mark the transition between the glacial diamictites and the overlying cap carbonates. This study deals with the suggestion that a large-scale impact event might have triggered the rapid deglaciation.

Here we discuss the search for impact signatures using mineralogical and geochemical methods in samples from the Chuos/Rasthof (Sturtian) and Ghaub/Maieberg (Marinoan) postglacial transition at the Neoproterozoic Otavi Group (Namibia). However, no geochemical and mineralogical signatures that would be characteristic of an impact, such as an enrichment in siderophile element abundances or the presence of Cr-spinels or shocked minerals, were detected in our samples. Thus, there is no indication yet that an impact event was involved in the formation of the studied transition layers.

Mindestens zwei globale neoproterozoische Vereisungsereignisse ("Schneeball Erde"/"Snowball Earth") ereigneten sich im Cryogenium vor etwa 710 Ma (Sturtische Vereisung) und 635 Ma (Marinoische Vereisung), wobei die Ozeane entweder komplett zugefroren waren oder allenfalls einige kleine offene Wasseroasen verblieben. Weder die Ursache des Einsetzens der Vereisungen, sowie deren Verbreitung und Dauer, noch die Ursache der Abschmelzung werden derzeit hinreichend verstanden.

In dieser Studie versuchen wir an eine frühere Untersuchung unserer Arbeitsgruppe anzuschließen, die in den Gesteinseinheiten zwischen glazialen Diamiktiten und den darüber liegenden post-glazialen "Kappen"-Karbonaten (cap carbonates) auf das Vorhandensein einer extraterrestrischen Signatur hingewiesen hat. Die vorliegende Arbeit sucht nach Hinweisen auf die Möglichkeit, dass ein großes Impaktereignis das rasche Ende der Vereisung ausgelöst haben könnte.

Hier diskutieren wir die Suche nach Impaktsignaturen mittels mineralogischer und geochemischer Methoden in Proben aus postglazialen Übergangslagen der sturtischen Chuos/Rasthof und der marinoischen Ghaub/Maieberg Formationen in der neoproterozoischen Otavi Gruppe (Namibia). In unseren Proben konnten jedoch keine der für einen Impakt charakteristischen geochemischen und mineralogischen Signaturen, wie etwa eine Anreicherung an siderophilen Elementen beziehungsweise spezifische meteoritische Elementverhältnisse, oder die Anwesenheit von Cr-Spinellen oder geschockten Mineralen, nachgewiesen werden. Demnach gibt es bisher keine Anzeichen, dass ein Impaktereignis an der Entstehung der untersuchten postglazialen Übergangslagen beteiligt war.

1. Introduction

Neoproterozoic glaciations of global extent occurred within three different cryogenic periods: (1) the Sturtian (740–647 Ma, type location South Australia), (2) the Marinoan (660–635 Ma, type location South Australia), and (3) the Gaskiers (ca. 580 Ma, type location Avalonian Newfoundland, Canada), with the duration of each glaciation being estimated at several million years. The Snowball Earth hypothesis was introduced by Kirschvink (1992). A variety of hypotheses were suggested to explain the different global glaciations, such as the (i) Hard Snowball Earth – total ice coverage of oceans with rapid deglaciation (Hoffman et al., 1998; Hoffman and Schrag, 2002); (ii) Slushball Earth – without equatorial sea ice coverage and slower deglaciation (Harland, 1964; Hyde et al., 2000); the (iii) Zipper-rift model - climatic control of tectonic events based on diachronous rifting of Rodinia (Eyles and Janusczak, 2004); and (iv) high-tilt Earth – low latitudinal glaciations induced by seasonality based on higher obliquity (54°) (Williams, 2000).

Bodiselitsch et al. (2005) noted the presence of anomalously elevated contents of the element iridium in samples from the Sturtian and Marinoan diamictite/cap carbonate boundary layers at the Congo Craton and proposed that this anomaly reflects cosmic dust accumulation during the glaciation phase; furthermore, these authors used the abundance of Ir (and other siderophile elements) in the boundary layer to estimate the

duration of the glaciations, based on a steady-state accumulation of extraterrestrial dust. However, studies from other locations, in the Canadian Cordillera and in Namibia, have yielded ambiguous results. Peucker-Ehrenbrink and Hoffman (2006) noted slightly elevated abundances of osmium and a decrease in the $^{188}Os/^{187}Os$ isotopic ratio in samples from two continuously sampled profiles at the end of the Marinoan glaciation in Namibia (Otavi Platform) and the northern Canadian Cordillera (Mackenzie Mts.), where a 2-12 cm thick clay layer separates glacial diamictite from postglacial cap dolomite. On the other hand, further analyses of additional samples, and re-analysis of a split of the Congo Craton sample, by Waters et al. (2009, 2010) failed to find significant platinum-group element (PGE) anomalies, but confirmed the Os isotopic trend. They also noted that samples with higher Os concentrations have less radiogenic Os, which is consistent with binary mixing between terrestrial and extraterrestrial Os. This either means that the Ir anomaly found by Bodiselitsch et al. (2005) is not global or not of purely extraterrestrial origin. Recently, Ivanov et al. (2013) tried to test the cosmic dust deposition hypothesis on the Ediacaran Period. However, the PGE concentrations were at the background level, which they interpreted as an indication that the Ediacaran glaciations were either not of Snowball but more likely of Slushball Earth conditions or that the Snowball Earth phase was of very short duration so that not enough PGEs could have accumulated.

Koeberl et al. (2007a, b) proposed an alternative explanation, namely that the Ir anomaly was the result of an impact event. Kring (2003) already argued about possible effects of impact events on the termination of Snowball Earth conditions, and suggested quantitative modeling of the vapor plume effects. The goal of the present paper is to investigate if it is conceivable that a large-scale impact event might have triggered the deglaciation. The problem of the climatic effects of large impact events is not clear, as previously a Chicxulub-scale impact was suggested to induce global freezing. In terms of cratering rates, it is statistically plausible that the impact of a ~5 km diameter asteroid occurs during a “snowball period” with duration of several million years. Most probable is an impact into the ice-covered ocean. In such a case a vapor plume with a total mass of several times 10^{15} kg will rise up and then collapse over the atmosphere, creating a transient “hot spot”. The more indirect consequences may include a global enrichment of the upper atmosphere with water vapor, dust and sea salt particles (in

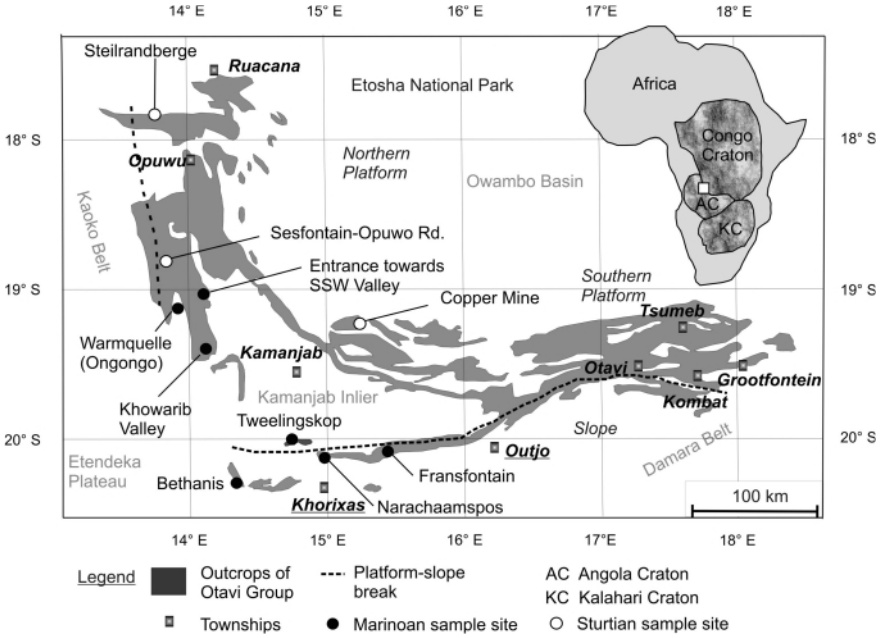

Figure 1: Geological map of Otavi group outcrops showing sampling sites of Sturtian and Marinoan postglacial transition layers (modified after Domack and Hoffman, 2011). The collected samples are listed in Table 1, including their lithology and facies.

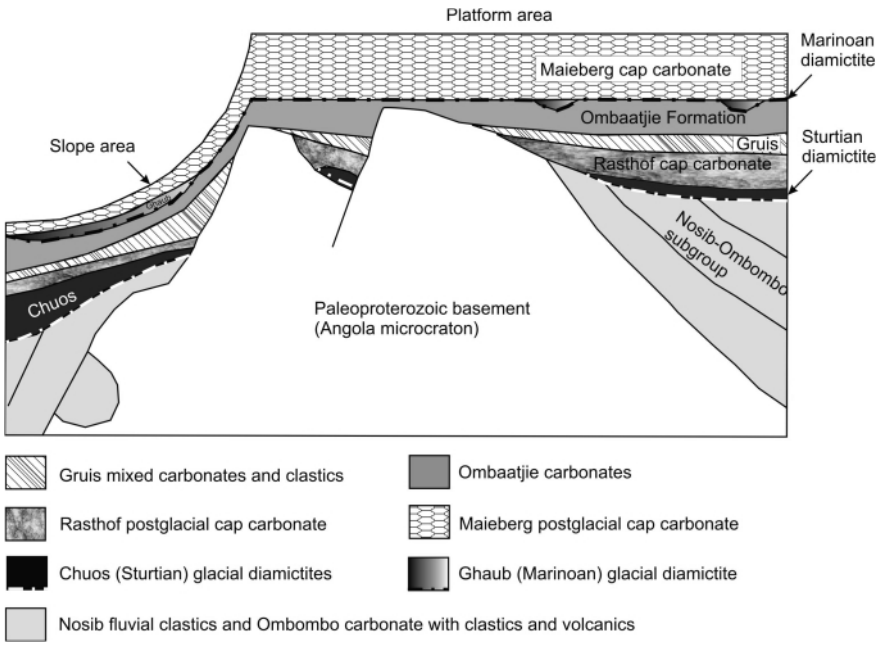

Figure 2: Geological cross section of Otavi Group (modified after Hoffman, 2005). Marinoan postglacial transition layer: sampling sites 1-7; Sturtian postglacial transition layer: sampling sites 8-10 (see Table 1 and Fig. 1 for details).

the case of an impact into the ocean). More detailed work, based on the initial studies reported by Koeberl et al. (2007a, b), is still necessary.

The aim of this study was, therefore, to search for evidence of an impact event in samples from the transition between the glacial diamictites and the overlying cap carbonates. The recognition of geological structures and ejecta layers on Earth as being of impact origin requires the detection of either shock metamorphic effects in minerals and rocks, and/or the presence of a meteoritic component in these rocks. In nature, shock metamorphic effects are uniquely characteristic of shock levels associated with hypervelocity impact. A wide variety of shock metamorphic effects have been identified, such as planar microdeformation features, optical mosaicism, changes in refractive index, birefringence, and optical axis angle, isotropization (e.g., formation of diaplectic glasses), and phase changes (high pressure phases; melting). Planar microstructures are the most characteristic expressions of shock metamorphism and occur as planar fractures (PFs) and planar deformation features (PDFs) in quartz and feldspar (see, e.g., Stöffler and Langenhorst, 1994; Montanari and Koeberl, 2000, French and Koeberl, 2010; Glass and Simonson, 2013; and references therein).

Another way to determine the impact origin of crater rocks or ejecta is by confirming the presence of a meteoritic component in these rocks. Meteoritic components have been identified for just fewer than 50 of the more than 180 impact structures that have so far been identified on Earth. The presence of a meteoritic component can be verified by measuring abundances and interelement ratios of the siderophile elements, especially the platinum group elements (PGE), which are much more abundant in meteorites than in terrestrial upper crustal rocks. For more detailed information on this topic, see, e. g., Koeberl (1998, 2014), Koeberl et al. (2012), and references therein.

Our research area, the Otavi Group in NW Namibia, is in the same geographical region as that of Bodiselitsch et al. (2005); both are located in the Congo Craton. Hence, we undertook a search for impact signatures in samples from the Sturtian and Marinoan “boundary clay” similar to those found in distal impact ejecta, such as the Late Eocene or the Cretaceous/Paleogene boundary (cf. Montanari and Koeberl, 2000).

A Site No.*	Sample No.	Sub samples	Locality	GPS Data	Lithology	Glaciation/Deglaciation Event	Facies
1	C 1	C 1a	Fransfontain	20°11'59.06"S; 15° 0'58.68"E	allodapic dolostone	Ghaub-Maieberg Fm.	slope
1		C 1b	Fransfontain	“	allodapic dolostone	Ghaub-Maieberg Fm.	slope
1		C 1c	Fransfontain	“	allodapic dolostone	Ghaub-Maieberg Fm.	slope
2	C 2	C 2a	Narachaamspos	20°11'27.68"S; 14°51'4.42"E	boundary layer	Ghaub-Maieberg Fm.	slope
2		C 2a-01-17 (17)	Narachaamspos	“	boundary layer/cap carbonate	Ghaub-Maieberg Fm	slope
2		C 2b	Narachaamspos	“	boundary layer	Ghaub-Maieberg Fm.	slope
2		C 2c	Narachaamspos	“	boundary layer	Ghaub-Maieberg Fm.	slope
2	C 3	C 3_1	Narachaamspos	20°11'28.74"S; 14°51'4.38"E	boundary layer	Ghaub-Maieberg Fm.	slope
2		C 3_2	Narachaamspos	“	boundary layer	Ghaub-Maieberg Fm.	slope
2	C 17	C 17a	Narachaamspos	no data	tectonic clay	Ghaub-Maieberg Fm.	slope
2		C 17b	Narachaamspos	no data	ashy clay	Ghaub-Maieberg Fm.	slope
2		C 17c	Narachaamspos	20°11'28.00"S; 14°51'2.76"E	boundary layer	Ghaub-Maieberg Fm.	slope
3	C 4		Tweelingskop	20° 7'13.47"S; 14°35'1.30"E	red dolomite	Ghaub-Maieberg Fm.	platform edge
3	C 5		Tweelingskop	20°7'13.82"S; 14°35'1.71"E	aeolianite	Ghaub-Maieberg Fm.	platform edge
4	C 6		Bethanis	20°24'24.00"S; 14°20'13.55"E	red Silt	Ghaub-Maieberg Fm.	distal slope
4	C 7		Bethanis	20°7'13.47"S; 14°35'1.30"E	dolomite rhythmite	Ghaub-Maieberg Fm.	distal slope
5	C 14	C 14a	Entrance to SW Valley	19°11'18.40"S; 13°56'13.39"E	red diamictite	Ghaub-Maieberg Fm.	platform
5		C 14b	Entrance to SW Valley	“	red transition Layer	Ghaub-Maieberg Fm.	platform
5		C 14c	Entrance to SW Valley	“	tectonized clay	Ghaub-Maieberg Fm.	platform
5		C 14d	Entrance to SW Valley	“	red-green boundary clay	Ghaub-Maieberg Fm.	platform
5		C 14e	Entrance to SW Valley	“	basal dolomite	Ghaub-Maieberg Fm.	platform
5	K4 profile	K4-01-08 (8)	Entrance to SW Valley	“	basal dolomite	Ghaub-Maieberg Fm.	platform
6	C 15	C 15a	Khowarib Valley	19°18'24.52"S; 13°59'25.57"E	banded cap-dolomite	Ghaub-Maieberg Fm.	platform
6		C 15b	Khowarib Valley	“	boundary layer	Ghaub-Maieberg Fm.	platform
6		C 15c	Khowarib Valley	“	red boundary clay	Ghaub-Maieberg Fm.	platform
6		C 15d	Khowarib Valley	“	basal cap dolomite	Ghaub-Maieberg Fm.	platform
6		C 15e	Khowarib Valley	“	boundary clay	Ghaub-Maieberg Fm.	platform
6	P49 profile	P49-01-18 (15)	Khowarib Valley	“	basal cap dolomite	Ghaub-Maieberg Fm.	platform
7	C 16	C 16a	Ongongo (Warmquelle)	19°8'35.77"S; 13°51'15.40"E	sericitized clay	Ghaub-Maieberg Fm.	platform
7		C 16b	Ongongo (Warmquelle)	“	basal mylonite	Ghaub-Maieberg Fm.	platform
7		C 16c	Ongongo (Warmquelle)	“	opalized layer	Ghaub-Maieberg Fm.	platform
7	K2 profile	K2-01-11 (11)	Ongongo (Warmquelle)	“	basal cap carbonate	Ghaub-Maieberg Fm.	platform

B Site No.*	Sample No.	Sub samples	Locality	GPS Data	Lithology	Glaciation/Deglaciation Event	Facies
8	C 8		Copper Mine	19°25'18.43"S; 15° 9'50.90"E	red carbonate	Chuos- Rasthof Fm.	platform
8	C 9		Copper Mine	“	carbonate-quartzite	Chuos- Rasthof Fm.	platform
8	C 10	C 10_1	Copper Mine	“	sandstone	Chuos- Rasthof Fm.	platform
8		C 10_2	Copper Mine	“	sandstone compact	Chuos- Rasthof Fm.	platform
9	C 12		Steilrandberge	17°47'1.67"S; 13°39'54.10"E	red-brown dolomite	Chuos- Rasthof Fm.	platform
10	C 13	C 13a	Sesfontain-Opuwo Rd	18°46'26.49"S; 13°45'11.24"E	brown sandstone unaltered	Chuos- Rasthof Fm.	platform
10		C 13b	Sesfontain-Opuwo Rd	“	red/green sandstone altered	Chuos- Rasthof Fm.	platform
10		C 13c	Sesfontain-Opuwo Rd	“	transition zone to carbonate	Chuos- Rasthof Fm.	platform

*For site number localities see Fig. 1.

Table 1: Locality of sample sites and sample description of Ghaub (Marinoan) Fm. (A) and Chuos (Sturtian) Fm. (B)

2. Geological background

The research area is located in the Neoproterozoic Otavi Group in NW-Namibia (Fig. 1). The Otavi Platform formed along the southern fringe of the Congo Craton and abuts on the continental slope further south and west. These predominantly calcareous sedimentary successions, uni-

fied as Otavi Group, are located in a foreland position relative to the Kaoko Belt in the west and the Damara Belt in the south (Hoffman, 2002, 2005; Fig. 1, 2). The Otavi Group is subdivided into three subgroups, which are separated from each other by two glaciogenic diamictite units, the lower Chuos Formation and the upper Ghaub Formation (Hoffman, 2002, 2005; Fig. 2).

Continental break-up of the Mid-Proterozoic Rodinia Supercontinent produced world-widespread extensional rift systems followed by the development of passive continental margins. On the Congo Craton initial rifting caused deposition of siliciclastic sediments (conglomerate, arkosic quartzite, and siltstone with minor shale and carbonate, Hedberg, 1979); later subsidence and transgression led to the development of an enormous epicontinental platform area with paleo-climatic and oceanographic influenced sea-level fluctuation, where the thick sequence of Otavi Group carbonate dominated the accumulated sediments.

The middle Otavi Group is bounded by two discrete intervals of diamictite and associated by glaciomarine deposits, sandwiched by thick carbonate piles. The glaciogenic origin of the older interval (Chuos Formation) was first documented by Martin (1965) and Hedberg (1975). Later, Hoffmann and Prave (1996) lined out the younger glaciogenic interval (Ghaub Formation), covering an erosional surface on top of a carbonate platform sequence (Ombaatjie Formation). The sediments of both glaciogenic periods are overlain by distinct “cap-carbonate” layers, represented by the basal parts of the Rasthof- and Maieberg formations. The upper Otavi Group (Tsumeb Subgroup) is a thick and rather monotonous stack of grainstone-dominated cycles of cherty dolomite, deposited during the prolonged drift stage of the Panafrican Damara orogenic cycle.

3. Samples and methods

Our samples were collected from postglacial transition layers between the Chuos- and Rasthof formations. (Sturtian ice age) (5 bulk samples and 6 subsamples – total 9 from 3 locations), as well as between the Ghaub- and Maieberg formations. (Marinoan ice age) (11 bulk samples and 4 profiles – total 79 samples from 7 locations) of the Neoproterozoic Otavi Group in NW-Namibia (Fig. 1, Table 1AB). The methods used in this study are given in Table 2.

The mineralogical composition of our samples was studied using the petrographic microscope, X-ray powder diffraction (XRD), cathodoluminescence microscopy (CL), and micro-Raman spectroscopy at the University of Vienna. Instrumental neutron activation analysis (INAA) and X-ray fluorescence (XRF) spectrometry, as well as analytical electron microscopy (AEM), were used for geochemistry.

XRD data were collected at with a Phillips-diffractometer (PW 3710, goniometer PW-1820), CuKα radiation (45 kV, 35 mA), step size of 0.02 degrees, and counting time of 1 s per step. Minerals were identified using the Joint Committee on Powder Diffraction Standards database (JCPDS, 1980). Also, the clay fraction was measured by XRD.

A Renishaw RM1000 confocal edge filter-based micro-Raman spectrometer with 20 mW, 632.8 nm He-Ne laser excitation system, and thermoelectrically cooled charged coupled device array detector was used at the Institute of Mineralogy and Crystallography, University of Vienna, for identification of some mineral phases. For identification of different generations of carbonate cement and

Sample Nr*	Petrography	CL	Raman	XRD	XRD clay	XRF (major elements)	XRF (trace elements)	INAA	INAA clay	Mineral separation (decarbonatized sieved fractions)	SEM/EDX
C 1a	X			X	X		X	X	X	X	
C 1b	X	X		X	X		X	X	X	X	
C 1c	X			X		X	X	X			
C 2a	X	X	X	X	X		X	X	X	X	
C 2b				X	X		X	X	X	X	
C 2c				X	X		X	X	X	X	
C 3_1	X			X	X		X	X	X	X	
C 3_2	X	X		X	X		X	X	X	X	X
C 4	X		X	X			X	X	X		
C 5	X	X		X	X	X	X	X	X	X	
C 6	X			X	X		X	X	X	X	
C 7	X			X	X		X	X	X	X	
C 8	X	X		X	X		X	X	X	X	
C 9	X			X	X	X	X	X	X	X	X
C 10_1	X			X	X	X	X	X	X	X	
C 10_2	X			X	X	X	X	X	X	X	
C 12	X		X	X	X	X	X	X	X	X	
C 13a	X			X	X	X	X	X	X	X	X
C 13b	X		X	X	X	X	X	X	X	X	X
C 13c	X			X	X		X	X	X	X	X
C 14a	X	X		X	X		X	X	X	X	
C 14b				X	X	X	X	X	X	X	
C 14c				X	X	X	X	X	X	X	
C 14d	X			X	X		X	X	X	X	
C 14e	X			X	X		X	X	X	X	
C 15a	X										
C 15b				X	X	X	X	X	X	X	
C 15c	X			X		X	X	X			
C 15d	X	X		X		X	X	X			
C 15e	X			X			X	X	X	X	X
C 16a				X		X	X	X			
C 16b	X			X		X	X	X	X	X	X
C 16c	X			X		X	X	X	X	X	X
C 17a				X		X	X	X	X	X	X
C 17b				X			X	X	X	X	X
C 17c	X	X		X			X	X	X	X	X
K2 profile (11)	X			X				X			
K4 profile (8)	X			X				X			
P49 profile (15)**	X			X				X			
C 2a profile (17)***	X	X						X			

* Legend: CL=cathodoluminescence microscopy, XRD=X-ray powder diffraction, XRF=X-ray fluorescence, INAA=instrumental neutron activation analysis, SEM/EDS=scanning electron microscopy – energy dispersive X-ray spectroscopy); ** petrography from 5 subsamples; *** petrography from 7 subsamples

Table 2: Methods used for sample characterization.

origin of quartz a Lumic HC5-LM CL-microscope was used. The acceleration voltage applied on the tungsten filament in the electron gun is 14 kV; the beam current can be varied from about 0.05 to 0.4 mA, depending on the examined material.

INAA was used for the determination of the contents of major and trace elements, from which some were selected for this study (Cr, Co, Ni, Au, and Ir). For this purpose, approximately 150 mg of each of the powdered samples were weighed and sealed in small polyethylene vials, as well as about 60–100 mg of three of the following international rock standards: the carbonaceous chondrite Allende (Smithsonian Institution, Washington DC, USA; Jarosewich et al., 1987), the granite AC-E (Centre de Recherche Pétrographique et Géochimique, Nancy, France; Govindaraju, 1989), and the Devonian Ohio shale SDO-1 (United States Geological Survey; Govindaraju, 1989). These capsules were irradiated in the 250 kW Triga Mark II reactor at the Atominstitut (Institute of Atomic and Subatomic Physics) of the Technical University of Vienna for 6–8 h at a thermal neutron flux of about $1.7*10^{12}$ n $cm^{-2}s^{-1}$. Three measurements cycles, according to the halflives of the nuclides, were done using high purity germanium detectors with relative efficiencies of about 40 to 45 % and energy resolutions of 1.76 – 1.82 keV at 1332 keV (^{60}Co), respectively. For further details on the INAA measurements, see Mader and Koeberl (2009).

XRF analyses were done using a Philips PW 2400 sequential X-ray spectrometer equipped with a Rh-excitation source (Department of Lithospheric Research, University of Vienna), where the contents of the main elements and some selected trace elements were measured and considered in this study. The specimens were ground in an electric agate mill, homogenized, dried at 110 °C and fired at 950 °C to determination of water content and loss on ignition. For XRF analyses, fused beads were produced consisting of a 1:5 mixture of fired sample material and flux ($Li_2B_4O_7$).

Polished smeared slides were carbon-coated and examined at the Department of Mineralogy, Natural History Museum, Vienna (Austria) on a JEOL JSM 6400 SEM equipped with an energy-dispersive X-ray (ED) analyzer.

Detrital minerals are dispersed in dominant carbonate matrix. Thus, the crushed sample materials were treated with formic acid in order to dissolve carbonate minerals. Thereafter the remaining detrital grains were sieved and the grain size fractions between 63 and 400 micrometers were studied under the binocular microscope in order to check the minerals present for potentially enclosed grains of shocked quartz, impact spherules or chromium spinels. To retrieve possible Cr-spinel grains, the ferrimagnetic minerals were segregated using a Frantz Isodynamic magnetic separator. Within the resulting magnetic fractions, no Cr-spinel grains were found; however, the presence of magnetites and pyrites was determined from to their crystal shapes. The identity of some rounded magnetic grains (samples C3_2, C17a, C7) could not be determined under the binocular microscope; thus thick sections were prepared for SEM-EDS studies.

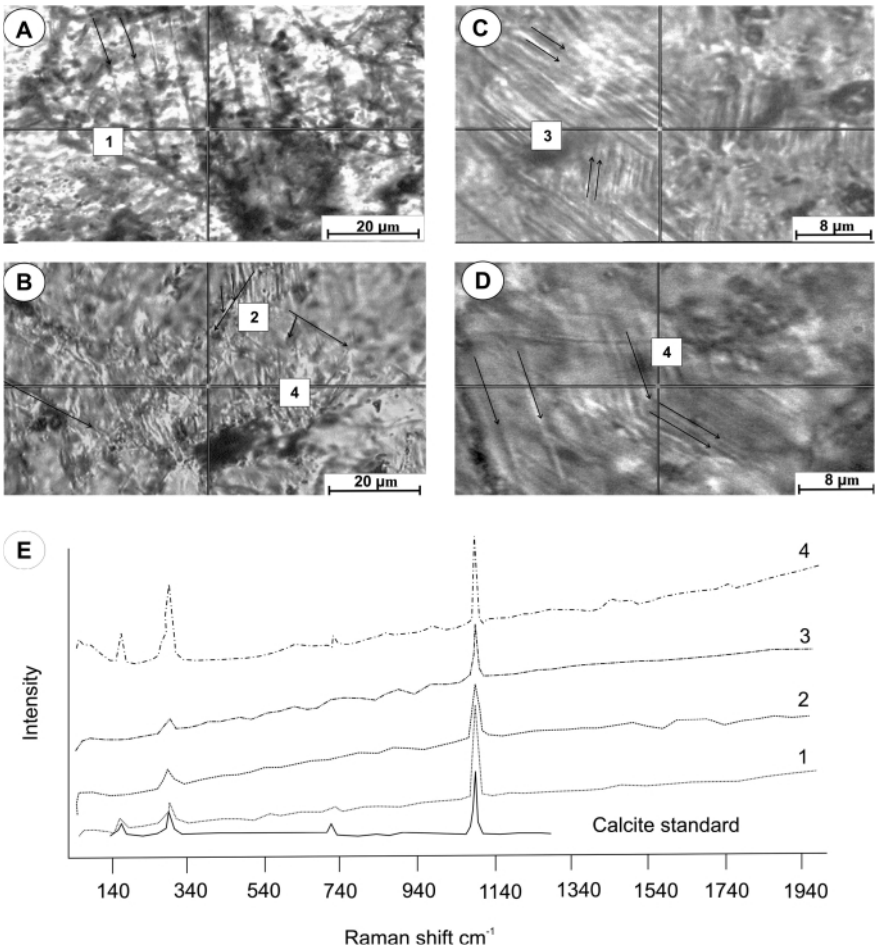

Figure 3: Raman spectra of densely twinned calcite and thin section photos of K2-1 and K4-1 samples showing measuring points. The Raman spectra are marked by numbers (1-4), and measuring points are shown on thin section photos (plain polarized lights). (A) normal mechanical twins in K4-1 sample; (B) in sample K2-1 the mechanical twins are crossed by a closely spaced set of lamellae that do not appear to represent shock deformation lamellae. (C) closely spaced sets of lamellae with two orientations in a calcite grain in the sample K4-1; (D) closely spaced sets of lamellae with two orientations in a calcite grain in the sample K2-1. The orientations of lamellae sets are marked by arrows.

4. Results

4.1 Optical microscopy and XRD: search for shocked quartz

As some of the most important mineralogical indicators of shock metamorphism are PFs and PDFs in

quartz (cf. Stöffler and Langenhorst, 1994; French and Koeberl, 2010), we studied 60 thin sections and 12 smear slides by optical microscopy, and found mostly carbonate minerals in both the diamictite and the boundary layers. The diamictites were either fine-grained or micritic-clayish material with carbonate clasts. The Sturtian and Marinoan transition layers contain only authigenic material (hematite, sericite). Only a few Sturtian and Marinoan transition samples contain a low amount (5 vol%) of detrital minerals (feldspar, mica). The Sturtian basal carbonate contains coarse detrital mineral phases between and in the cores of oncoids.

The Marinoan Narachaamspos transition layer (sample C2a) contains a few diamictite layers with coarse-grained quartz, calcite, K-feldspar, and mica. At this location orthoclase, microcline, and albite are twinned, and mica is kink-banded. No shock deformation was observed in the quartz grains.

The basal carbonate from the Bethanis location (sample C7) also contains coarse detrital phases, especially chlorite and quartz. Several chlorites were kinked, but quartz grains do not contain any signature of shock deformation. The material of Sturtian and Marinoan postglacial layers are fine-grained, where the quartz occurs as secondary phase: cement among synsedimentary structures (C3 at Narachaamspos), and as fracture-filling material (e.g., K2, K4, P49 Marinoan cap carbonate profiles). Several carbonate grains in samples K4 and K2 contain dense, differently oriented deformation lamellae systems (Fig. 3).

CL microscope studies were used to distinguish authigenic and detrital quartz and to determine other detrital phases. We searched for shock deformation lamellae in quartz using CL, but did not find any characteristic signatures such as described by, e.g., Boggs et al. (2001) and Hamers and Drury (2011). In our CL studies, quartz grains show no luminescence color, indicating a diagenetic origin of the quartz in the Sturtian and Marinoan postglacial transition layers. As a result of tectonic overprint sigmaclasts were observed in Marinoan postglacial basal cap carbonate (C2a profile).

Samples from Tweelingskop (C4) which are also related to the Marinoan period, have high quartz contents due to their deposition in karstic environments at the outer platform edge and basal cap carbonate from Narachaamspos also contains abundant quartz, but in that case was deposited as turbidity current in slope facies environments. Quartz lenses within these samples do not show luminescence color, indicating a

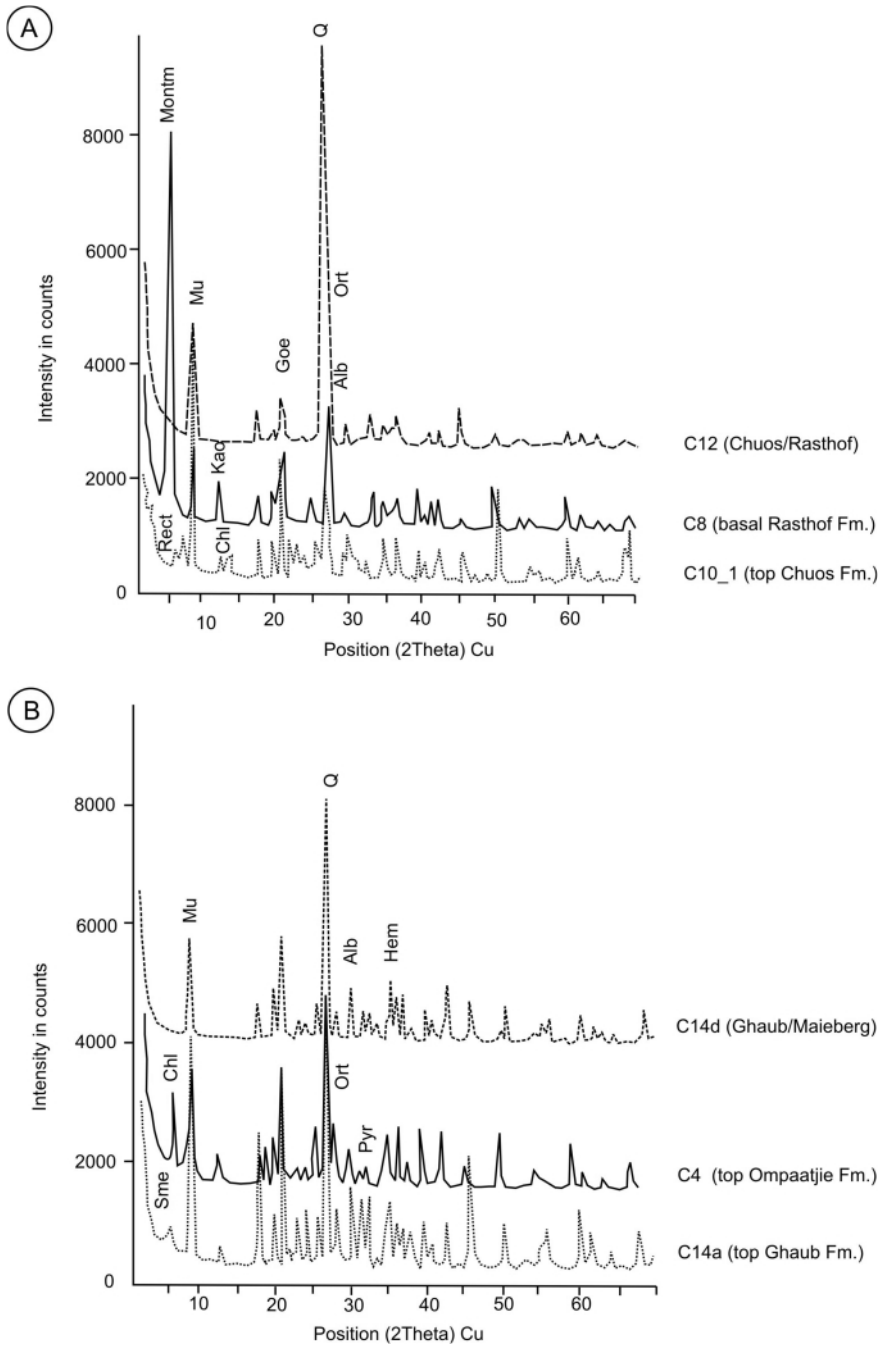

Figure 4: Selected XRD spectra of Sturtian (A) and Marinoan (B) stratigraphic sections after dissolving carbonate with formic acid. All of presented Sturtian and Marinoan layers contain quartz (q) and muscovite (mu). (A) Sturtian top diamictite (C10_1) contain different clay mineral phases (montmorillonite (mont), chlorite-chl, rectorite-rect, kaolinite-kao), which are derived by clay minerals. Sturtian postglacial transition layer (C8, C12) contains goethite (goe) and feldspar (alb, ort). The Marinoan transition layers (B) contain hematite (hem) (C14), smectite (sme) (C14a), feldspar (alb, ort) (C4, C14d) pyrite (pyr) and chlorite (chl) (C4).

tectono-metamorphic overprint with collateral quartz-mobilization and recrystallization. In the EDS spectra, the presence of Fe and Si was noted, indicating hematite-magnetite coating on quartz. Chrome spinels were not noted in the XRD spectra of the clay fractions; only feldspars (albite, orthoclase), quartz, muscovite, hematite, goethite and clay minerals, such as chlorite, smectite, and kaolinite, were found (Fig. 4AB).

4.2 Geochemistry

The most important geochemical signature of a meteoritic component is an enrichment in the contents of siderophile elements (and other related elements that are also enriched in meteorites) in ejecta samples compared to contents in the average upper continental crust (see above). In our analyses, the contents of the elements Cr, Ni, and Co do not show any significant enrichment. The abundances of Ir were all below the detection limit oif INAA (1-2.5 ppb). It should be noted that the sensitivity of our Ir analyses was not as good as that of the Bodiselitsch et al. (2005) study.

The Ni/Cr and Co/Cr ratios for the transition layer samples from Narachaamspos (C2a-c, C17a, C3-1-2) Sesfontain-Opuwo Rd (C13a-b), Steilrandberge (C12, C12a), Bethanis (C6), and Entrance to the SW-Valley (C14 b, d1, e) are near or higher than values for the upper continental crust (Rudnick and Gao,

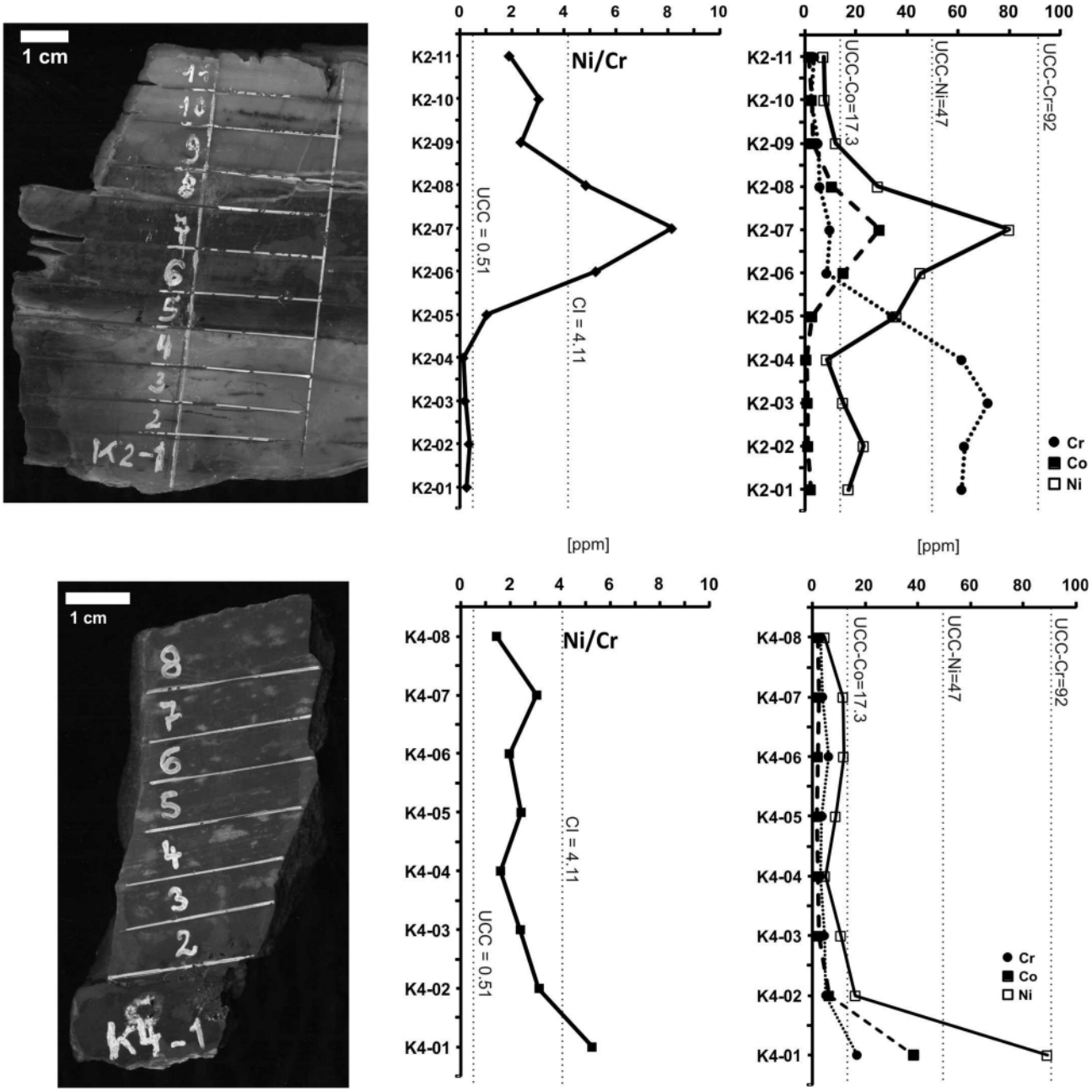

Figure 5: Cr-Ni-Co values and Ni/Cr ratio profiles of Marinoan cap carbonate profile from Warmquelle (K2) and Entrance to the SW Valley (K4). The boundary layers are slightly enriched in Ni/Cr, Ni, Cr, Co values compared to upper continental crust (Rudnick and Gao, 2003) but the Ni/Cr ratio of samples K4-01, K2-06, K2-07, K2-08 is higher than that of chondritic meteorites (Henderson and Henderson, 2009), not indicating the presence of a meteoritic component.

2003) for both of bulk rock samples and their clay fractions after dissolving the carbonate (Fig. 5).

5. Discussion

Koeberl et al. (2007a, b) suggested that the impact of an asteroid onto the ice-covered planet might lead to a deglaciation of the Snowball Earth, although details remained open. Thus a search for possible evidence of any impact ejecta debris in post-glacial transition layers would be one possibility to find evidence for such a hypothesis. However, no impact crater or impact ejecta have been detected, which formed during the Snowball Earth glaciation or deglaciation. Several impact craters have been dated near the Cryogenian Period, but their ages are not very accurately known (Strangways 646 ± 42 , Söderfjärden ~ 600, Beaverhead ~ 600, Saarijärvi > 600, Jänisjärvi 700 ± 5 million years old; cf. Earth Impact Database, 2014). In addition, all these craters are relatively small, from 6 to 60 km diameter.

In a search to confirm the Ir anomalies detected by Bodiselitsch et al. (2005) at other locations, Peucker-Ehrenbrink and Hoffman (2006) indeed detected elevated (relative to crustal abundances) Os concentrations with a lower than crustal radiogenic Os isotopic component for Marinoan postglacial transition layers in Canadian Cordillera, revealing a possible mixture of terrestrial and extraterrestrial Os. But Waters et al. (2009, 2010) measured platinum group element (PGE) abundances and Re-Os isotope systematics of two continuous Marinoan deposits from the Otavi Platform and Hoanib Shelf basin in northwestern Namibia and found mostly crustal-level Os concentrations for both sections (5.0-74 ppt), with a lack of significant anomalies. One sample from the Hoanib Shelf basin is an exception, with an Os concentration of 0.7 ppb. In their analyses, osmium concentrations vary inversely with sediment accumulation rates, and samples with higher Os concentrations have less radiogenic Os, which is consistent with binary mixing between terrestrial and extraterrestrial Os, similar to what was found by Peucker-Ehrenbrink and Hoffman (2006). Nevertheless, no

Location	Fransfontain			Tweelingskop		Bethanis	
Strat. setting	M	G/M	G/M	O	G	G/M	M
wt. % / sample	C1a	C1b	C1c	C4	C5	C6	C7
ppm							
Cr	7.22	15.0	25.8	14.4	9.27	14.1	30.8
Co	1.32	5.43	7.20	2.14	3.50	4.03	6.82
Ni	7.1	47.1	67.7	7.1	20.9	34.3	53.9
Au (ppb)	<0.2	0.2	0.2	<0.5	<0.4	<0.2	0.1
Ir (ppb)	<0.4	<0.5	<1.6	<0.7	<0.6	<0.6	<1.4

Location	Narachaamspos							
Strat. setting	G	G/M	G/M	G/M	G/M	G	G/M	M
sample	C 2a	C 2b	C 2c	C 3_1	C 3_2	C17a	C17b	C17c
ppm								
Cr	20.2	65.4	35.4	94.1	110	191	88.5	41.4
Co	18.2	32.7	16.9	40.7	56.9	2.93	7.04	14.0
Ni	93.0	132	128	172	257	48.2	82.1	63.6
Au (ppb)	<1.0	<1.1	<0.9	0.5	<0.9	<0.7	0.3	<0.9
Ir (ppb)	<1.1	<1.1	<1.7	<1.9	<1.9	<2.3	<1.7	<0.9

Location	Narachaamspos							
Strat. setting	G	G/M	G/M	G/M	G/M	G	G/M	M
sample	C 2a1-T	C 2b-T	C 2c-T	C 3_1-T	C 3_2-T	C 17a-T	C 17b-T	C 17c-T
ppm								
Cr	56.0	232	120	131.	93.0	129	98.3	89.1
Co	15.8	33.2	17.0	16.4	26.9	2.11	1.64	6.98
Ni	115	250	184	241	192	112	131	98.2
Au (ppb)	0.37	<1.4	<0.7	<1.1	<1	<1.1	<0.92	<0.6
Ir (ppb)	<1.3	<2.2	<1.7	<2.0	<1.8	<2.2	<0.92	<2.6

Location	Entrance to the SW Valley						
Strat. setting	G	G/M	G/M	G/M	G/M	G/M	M
sample	C 14a	C 14b	C 14c	C 14d	C 14d1	C 14d2	C 14e
ppm							
Cr	32.4	5.08	44.8	71.3	26.2	71.7	12.2
Co	3.79	3.28	5.93	4.83	62.2	4.87	12.2
Ni	26.7	6.5	43.2	75.0	139	51.8	27.8
Au (ppb)	0.5	<0.3	<0.5	1.1	0.8	<0.6	0.3
Ir (ppb)	<1.0	<0.5	<1.3	<2.3	<1.4	<1.7	<1.0

Location	Entrance to the SW Valley				
Strat. setting	G	G/M	G/M	G/M	M
wt. %	C 14a-T	C 14b-T	C 14c-T	C 14d-T	C 14e-T
ppm					
Cr	158	133	111	65.4	32.4
Co	4.39	7.80	6.47	49.2	22.5
Ni	122	97.5	128	206	109
Au (ppb)	<0.8	0.7	<0.8	0.9	0.7
Ir (ppb)	<2.3	<1.9	<1.8	<2.4	<1.2

Location	Khowarib Valley					Warmquelle		
Strat. setting	G/M	G/M	M	G/M	M	G	G/M	M
wt. % / sample	C 15b	C 15c	C 15d	C 15e	C 15e1	C 16a	C 16b	C 16c
ppm								
Cr	26.9	24.6	73.7	40.0	3.42	151	25.3	59.8
Co	3.38	2.60	6.69	11.6	2.68	9.68	3.49	0.75
Ni	11.3	23.1	40.2	34.6	<19	62.9	18.3	11.7
Au (ppb)	<0.3	<0.4	<0.6	<0.9	<0.4	<0.9	0.6	0.2
Ir (ppb)	<1.3	<0.9	<1.4	<1.2	<1.1	<2.0	<0.6	<1.2

Location	Fransfontain		Tweelingskop		Bethanis		Khowarib Valley		Warmquelle	
Strat. setting	M	G/M	O	G	G/M	M	G/M	G/M	G/M	M
sample	C 1a-T	C 1b-T	C 4-T	C 5b-T	C 6-T	C 7-T	C 15b-T	C 15e-T	C 16b-T	C 16c-T
ppm										
Cr	95.9	84.4	110	16.8	23.1	86.7	127	68.1	87.0	70.3
Co	13.0	12.5	5.39	2.19	7.95	21.0	7.54	9.30	4.37	2.00
Ni	147	288	55.1	16.1	78.1	275	49.5	81.2	96.2	48.8
Au (ppb)	2.3	<1	0.4	0.2	<0.8	<0.9	<0.9	0.8	1.6	0.6
Ir (ppb)	<1.5	<1	<2.9	<0.75	<1.2	<1.6	<0.95	<2.3	<1.5	<1.3

Table 3: Major and trace element contents for post-glacial transition samples from Namibia.
A) Marinoan transition layers.
Legend: G= Ghaub Fm., G/M = Ghaub/Maieberg boundary, M= Maieberg Fm., C=Chuos Fm., C/R= Chuos/Rasthof boundary, R= Rasthof Fm., O=Ombaatjie Formation Clay fractions are marked by "T". LOI = loss on ignition. "n.d." = not determined. The Ir content is below the detection limit for all samples (1-2.5 ppb). -- = some of the major element contents were not determined.

distinct and unambiguous PGE or Os isotope signal was found, making a global presence of an extraterrestrial anomaly in Sturtian and Marinoan postglacial transition layers less likely.

As noted above, impact ejecta should contain evidence of shock metamorphism or the geochemical or mineralogical signature of an extraterrestrial component (cf. Montanari and Koeberl, 2000; Cavosie et al., 2010; French and Koeberl, 2010; Koeberl et al., 2012). Our postglacial boundary layer samples do not contain any high pressure phases, chrome spinels, or geochemical impact signatures (Table 3, Figs. 3-6). In ejecta layers, the shocked minerals should be a primary phase, and not have formed by secondary processes, such as diagenesis. Quartz, feldspar, and muscovite were identified as detrital minerals in our samples, with feldspar grains starting to be altered to kaolinite. Several locations, Narachaamspos (Marinoan, samples C3_1, C3_2) and Copper Mine (Sturtian, sample C8) contain coarser fragments of detrital minerals (quartz pebble - 3 mm, feldspar - 0.1 mm), which contain neither shock lamellae (PDF) or planar fractures (PF), nor high pressure minerals. In general, the quartz occurs as a secondary fracture filling phase, where no PDFs occur.

However, the mica and chlorite contain kink bends, but these may have formed by a successive tectono-metamorphic process. Little is known about shock deformation of calcite (e.g., Huson et al., 2009), but calcite can develop dense mechanical twins, which was noted in a few calcite grains in K2_1 and K4_1 sample (Fig. 3). Differently oriented dense deformation lamellae in carbonate occur in heterogeneous stress field at the time of deformation in sedimentary rock, so enhanced twin lamellae/mm in calcite probably indicate increased shear stress. Sigma clasts were observed in Marinoan postglacial basal cap carbonate (C2a profile), which can be explained by normal tectonic pressure.

The PGE abundances (e.g., Ir, Os) are below the detection limit (below 400 ppb for Os, and below 1.5-2.5 ppb for Ir) of INAA for our Sturtian and Marinoan postglacial transition layers; thus the detection limits here are worse than in the work of Bodiselitsch et al. (2005), who used coincidence counting INAA instead of normal INAA. It might of course be possible that any signature is in the sub-ppb range for Ir and Os; but the determination of such low abundances was beyond the scope of the present work. For a more detailed geochemical study, the PGE abundances in the clay fraction and of separated montmorillonites might have to be obtained, as well as Os or Cr-isotope data. In our samples the Cr, Co, Ni abundances were near (Marinoan: C3_1, C3_2, C17a-b, C2a-b, Sturtian: C9, C10) or below to the upper crustal values (Rudnick and Gao, 2003) (especially postglacial cap carbonates), and thus do not indicate any geochemical signature of impact ejecta (Table 3). Chrome spinels, as an impact marker mineral, also could not be identified in the silt fraction or in the coarser fraction with binocular microscopy and SEM-EDS analyses.

Thus, no unambiguous geochemical or mineralogical signature has been observed for meteoritic impact in Sturtian and Marinoan postglacial transition layers in Otavi Group, NW-Namibia.

Several Sturtian (C8, C10 from Copper Mine) and Marinoan (C14a, b-c –Entrance to the SW Valley) postglacial boundary layers contain smectite-rich clays (smectite, chlorite, rectorite, kaolinite). Smectite rich-clays can be formed by weathering of impact ejecta and fireball layer deposits (Ferrel and Dypvik, 2009). However, the smectite in our samples are derived from diagenesis and/or weathering of iron biomats or leaching, based on microtextural evidence.

Thus we can interpret our observations in two different ways:

1) There might have been an impact event at the end of one or both Snowball Earth glaciation periods, but no direct evidence is visible in our samples, at least not at our search level and precision. Some impact marker minerals might have been altered to clay minerals (smectite, rectorite, fine-grained chlorite), but this is clearly not confirming evidence of an impact event. The weathering of mineral fragments of meteorite minerals is a rapid process within the marine environment, where geochemical signatures can be changed due to diagenesis and alteration. Bodiselitsch et al. (2005) found Ir anomalies in samples from near to our research area, which did not appear at other locations of Neoproterozoic Snowball glaciations, making the “cosmic dust deposition” hypothesis difficult to confirm elsewhere. If an Ir anomaly occurs only at one outcrop of a marine stratigraphic section (Congo Craton – Bodiselitsch at al. 2005), a nearby marine impact could be postulated. But again, similar results would be expected at least within the same region. Only some admixture of extrater-

Location	Copper Mine				Steilrandberge		Sesfontain-Opuwo		
Strat. setting	R	C/R	C	C	C/R	R	C	C/R	R
sample	C 8	C 9	C 10_1	C 10_2	C 12	C 12a	C 13a	C 13b	C 13c
ppm									
Cr	8.52	66.2	61.0	74.3	15.2	4.57	26.4	37.6	11.3
Co	4.42	5.96	3.16	3.75	4.90	1.72	17.4	34.4	1.65
Ni	21.2	25.9	30.2	28.0	25.4	3.33	147	38.7	4.23
Au (ppb)	<0.5	0.4	0.4	<0.7	16.7	0.9	1.7	0.9	0.2
Ir (ppb)	<0.9	<1.3	<1.6	<1.5	<1.3	<0.6	<2.0	<1.6	<0.6

Location	Copper Mine				Steilrandberge	Sesfontain-Opuwo		
Strat. setting	R	C/R	C	C	C/R	C	C/R	R
sample	C 8-T	C 9-T	C 10-1-T	C 10_2-T	C 12-T	C 13a-T	C 13b-T	C 13c-T
ppm								
Cr	47.4	114	73.0	150	61.1	46.9	50.8	53.8
Co	18.8	6.31	3.85	9.37	12.8	16.5	24.4	23.5
Ni	59.4	95.4	40.2	63.2	67.8	146	72.5	173
Au (ppb)	0.7	0.6	<0.6	0.6	36.7	3.2	1.0	2.9
Ir (ppb)	<1.3	<2.0	<1.4	<3.9	<2.1	<2.5	<2.1	<1.2

Table 3: Major and trace element contents for post-glacial transition samples from Namibia. B) Sturtian transition layer.
Legend: G= Ghaub Fm., G/M = Ghaub/Maieberg boundary, M= Maieberg Fm., C=Chuos Fm., C/R= Chuos/Rasthof boundary, R= Rasthof Fm., O=Ombaatjie Formation Clay fractions are marked by “T”. LOI = loss on ignition. “n.d.” = not determined. The Ir content is below the detection limit for all samples (1-2.5 ppb). -- = some of the major element contents were not determined.

restrial material was indicated in samples from this region by the analyses of Waters et al. (2009, 2010), but our samples did not provide evidence for any significant extraterrestrial component; however, a small component might still exist, as our geochemical analyses had rather high detection limits. Nevertheless, no impact ejecta materials, such as shocked minerals, were found either.

2) There was no meteorite impact, and the minor Cr, Co, Ni enrichment was derived by iron-biomats or hydrothermal vents. The smectites are derived from diagenesis and/or weathering of iron biomats or leaching. The microtectonical and synsedimentary structures are derived by turbidite flow of rift basin, or post depositional tectonic processes or anchimetamorphosis during the diagenesis.

6. Conclusions

The lack of unambiguous mineralogical and geochemical signatures does not provide immediate support for any meteorite impact-induced deglaciation of the Sturtian and Marinoan glaciations. Other signatures, such as kinked mica, or dense lamellae in carbonate are common in normal tectonic pressure-temperature conditions. Even though smectite might be the derived by weathering of meteoritic minerals, the lack of any unambiguous impact evidence makes this unlikely. Further studies require more sensitive analytical methods, respectively better detection limits.

Location	Warmquelle profile										
Strat. setting	M	M	M	M	M	G/M	G/M	G/M	M	M	M
sample	K2-01	K2-02	K2-03	K2-04	K2-05	K2-06	K2-07	K2-08	K2-09	K2-10	K2-11
ppm											
Cr	61.5	62.5	71.8	61.5	34.3	8.63	9.80	5.89	5.17	2.53	3.8
Co	2.31	1.29	1.02	0.57	2.84	15.1	29.3	10.6	3.02	2.72	1.73
Ni	17.1	23.1	15.0	8.6	35.8	45.2	80.0	28.6	12.2	7.7	7.3
Au (ppb)	0.3	<0.4	<0.4	<0.3	0.2	<0.4	<0.4	<0.2	<0.2	0.1	0.1
Ir (ppb)	<1.1	<1.0	<0.9	<1.3	<1.1	<0.9	<1.0	<0.6	<0.3	<0.5	<0.5

Location	Entrance to the SW Valley Pofile							
Strat. setting	G/M	G/M	M	M	M	M	M	M
sample	K4-01	K4-02	K4-03	K4-04	K4-05	K4-06	K4-07	K4-08
ppm								
Cr	16.9	5.22	4.54	3.05	3.68	6.10	3.85	3.30
Co	38.5	6.45	2.39	2.01	1.88	2.20	2.41	2.06
Ni	89.1	16.5	11.1	4.9	8.9	11.9	11.8	4.7
Au (ppb)	0.4	2.3	0.3	<0.2	0.1	<0.2	<0.2	<0.2
Ir (ppb)	<0.8	<0.6	<0.5	<0.6	<0.5	<0.2	<0.2	<0.5

Location	Khowarib Valley profile						
Strat. setting	M	M	M	M	M	M	M
sample	P49-01	P49-02	P49-03	P49-04	P49-05	P49-06	P49-07
ppm							
Cr	3.40	2.22	1.89	1.93	1.74	2.05	1.52
Co	1.56	1.37	1.32	1.44	1.62	1.61	1.24
Ni	5.8	3.5	5.4	6.8	6.6	7.3	3.7
Au (ppb)	<0.2	<0.2	<0.2	<0.2	<0.2	<0.2	<0.1
Ir (ppb)	<0.2	<0.2	<0.2	<0.2	<0.2	<0.2	<0.1

Location	Khowarib Valley profile							
Strat. setting	M	M	M	M	M	M	M	M
wt. %	P49-08	P49-09	P49-11	P49-12	P49-13	P49-14	P49-16	P49-18
ppm								
Cr	1.80	1.68	1.59	1.63	1.58	1.57	2.50	1.54
Co	1.11	1.08	1.10	1.21	1.21	1.12	1.38	1.14
Ni	4.8	5.1	3.3	4.4	3.4	4.9	4.9	3.4
Au (ppb)	<0.2	0.1	<0.1	<0.1	<0.1	<0.2	<0.2	<0.2
Ir (ppb)	<0.2	0.05	<0.1	<0.1	<0.1	<0.2	<0.2	<0.2

Location	Narachaamspos								
Strat. setting	M	M	M	M	M	M	M	M	M
wt. %	C2a-01	C2a-02	C2a-03	C2a-04	C2a-05	C2a-06	C2a-07	C2a-08	C2a-09
ppm									
Cr	120	41.6	48.1	34.8	34.1	29.7	28.0	27.7	35.5
Co	14.6	7.46	6.71	12.6	6.34	5.63	4.43	5.39	12.5
Ni	99	79	99	120	79	62	57	56	53
Au (ppb)	<0.5	<0.4	<0.5	0.3	0.3	0.4	<0.4	0.3	0.4
Ir (ppb)	<1.8	<1.0	<1.5	<1.4	<1.4	<1.3	<1.3	<1.5	<1.2

Location	Narachaamspos							
Strat. setting	M	M	M	M	M	M	M	M
wt. %	C2a-10	C2a-11	C2a-12	C2a-13	C2a-14	C2a-15	C2a-16	C2a-17
ppm								
Cr	30.3	30	36.1	34.6	31.8	22.9	24.1	16.6
Co	4.84	7.11	7.10	11.7	17.2	7.58	20.4	26.7
Ni	56	61	69	102	132	43	76	142
Au (ppb)	0.2	0.8	0.6	1.0	0.4	0.2	6.0	0.2
Ir (ppb)	<1.3	<1.3	<1.3	<1.6	<1.4	<1.2	<1.3	<1.0

Table 3: Major and trace element contents for post-glacial transition samples from Namibia. C) Marinoan cap carbonates - profile.
Legend: G= Ghaub Fm., G/M = Ghaub/Maieberg boundary, M= Maieberg Fm., C=Chuos Fm., C/R= Chuos/Rasthof boundary, R= Rasthof Fm., O=Ombaatjie Formation Clay fractions are marked by "T". LOI = loss on ignition. "n.d." = not determined. The Ir content is below the detection limit for all samples (1-2.5 ppb). -- = some of the major element contents were not determined.

Acknowledgements

We are grateful to Peter Nagl (XRF), Lutz Nasdala, Eugen Libowitzky (micro-Raman spectroscopy), Susanne Gier (XRD), Lidia Pittarello, and Ludovic Ferriere (SEM) for help with lab work and helpful discussions, as well as to the reviewers for critical comments. This study was supported by the Austrian Academy of Sciences through a grant to C.K. (International Geological Correlation Program IGCP No. 512, work organization and sample export management. We appreciate the help of the reactor team of the Institute of Atomic and Subatomic Physics, Vienna, with the irradiations.

References

Bodiselitsch, B., Koeberl, C., Master, S. and Reimold, W.U., 2005. Estimating duration and intensity of Neoproterozoic Snowball glaciations from iridium anomaly. Science, 308, 239-242.

Boggs, S., Jr., Krinsley, D.H., Goles, G.G., Seyedolali, A. and Dypvik, H., 2001. Identification of shocked quartz by scanning cathodoluminescence imaging. Meteoritics and Planetary Science, 36, 783-791.

Cavosie, A.J., Quintero, R.R., Radovan, H.A. and Moser, D.E., 2010. A record of ancient cataclysm in modern sand: Shock microstructures in detrital minerals from the Vaal River, Vredefort Dome, South Africa. Geological Society of America Bulletin 122, 1968-1980.

Domack, E.W. and Hoffman, P.F., 2011. An ice grounding-line wedge from the Ghaub glaciation (635 Ma) on the distal foreslope of the Otavi carbonate platform, Namibia, and its bearing on the snowball Earth hypothesis. The Geological Society of America Bulletin, 123, 1448-1477.

Earth Impact Database: http://www.passc.net/EarthImpactDatabase/index.html, accessed May 26, 2014.

Eyles, N. and Januszczak, N., 2004. "Zipper-rift": a tectonic model for Neoproterozoic glaciations during the breakup of Rodinia after 750 Ma. Earth-Science Reviews, 65, 1-73.

Ferrell, R.E. and Dypvik, H., 2009. The mineralogy of the Exmore beds – Chickahominy Formation boundary section of the Chesapeake Bay impact structure revealed in the Eyreville core. In: G.S. Gohn, , C. Koeberl, K.C. Miller, and W.U. Reimold (eds.), The ICDP-USGS Deep Drilling Project in the Chesapeake Bay Impact Structure: Results from the Eyreville Core Holes. Geological Society of America Special Paper, 458, 723-746.

French, B.M. and Koeberl, C., 2010. The convincing identification of terrestrial meteorite impact structures: What works, what doesn't, and why. Earth-Science Reviews, 98, 123-170.

Glass, B.P. and Simonson, B.M., 2013. Distal Impact Ejecta Layers. A Record of Large Impacts in Sedimentary Deposits. Springer, Heidelberg, 716 pp.

Govindaraju, K. 1989. 1989 compilation of working values and sample description for 272 geostandards. Geostandards Newsletter, 13, 1-113.

Hamers, M.F. and Drury, M.R., 2011. Scanning electron microscope-cathodoluminescence (SEM-CL) imaging of planar deformation features and tectonic deformation lamellae in quartz. Meteoritics and Planetary Science, 16, 1814-1831.

Harland, W.B., 1964. Critical evidence for a great Infra-Cambrian glaciation. Geologische Rundschau, 54, 45-61.

Hedberg, R.M., 1975. Stratigraphy of the Owamboland basin, South West Africa. - Ph.D. thesis, Harvard University, Cambridge, MA, USA.

Hedberg, R.M., 1979. Stratigraphy of the Owamboland basin, South West Africa. Bulletin of Precambrian Research Unit, Cape Town, 24, 325 pp.

Henderson, P. and Henderson, G., 2009. The Cambridge Handbook of Earth Science Data. Cambridge University Press, Cambridge, UK, 286 pp.

Hoffman, P.F., 2002. Carbonates bounding glacial deposits: Evidence for Snowball Earth episodes and greenhouse aftermaths in the Neoproterozoic Otavi Group of northern Namibia. IAS Field Excursion Guidebook, 16th International Geology Congress, Rand Africaans Univ., Johannesburg, S-Africa.

Hoffman, P.F., 2005. 28th DeBeers Alex. Du Toit Memorial Lecture, 2004. On Cryogenian (Neoproterozoic) ice-sheet dynamics and the limitations of the glacial sedimentary record. South African Journal of Geology, 108, 557-576.

Hoffman, P.F. and Schrag, D. P., 2002. The Snowball Earth hypothesis: testing the limits of global change. Terra Nova, 14, 129-155.

Hoffman, P.F., Kaufman, A.J., Halverson, G.P. and Schrag, D.P., 1998. A Neoproterozoic Snowball Earth. Science, 281, 1342-1346.

Hoffmann, K.-H., and Prave, A.R., 1996. A preliminary note on a revised subdivision and regional correlation of the Otavi Group based on glaciogenic diamictites and associated cap dolostones. Communications of the Geological Society of Namibia, 11, 81-86.

Huson, S.A., Foit, F.F., Watkinson, A.J. and Pope, M.C., 2009. Rietveld analysis of X-ray powder diffraction patterns as a potential tool for the identification of impact-deformed carbonate rocks. Meteoritics and Planetary Science, 44, 1695-1706.

Hyde, W.T., Crowley, T.J., Baum, S.K. and Peltier, W.R., 2000. Neoproterozoic 'snowball Earth' simulations with a coupled climate/ice-sheet model. Nature, 405, 425-429.

Ivanov, A.V., Mazukabzov, A.M., Stanevich, A.M., Palesskiy, S.V., and Kozmenko, O.A., 2013. Testing the snowball Earth hypothesis for the Ediacaran. Geology, 41, 787-790.

Jarosewich, E., Clarke, R.S.J., and Barrows, J.N., 1987. The Allende meteorite reference sample. Smithsonian Contributions to the Earth Sciences, 27, 1-49.

JCPDS, 1980. Mineral Powder Diffraction File: Swarthmore (Joint Committee on Powder Diffraction Standards).

Kirschvink, J.L., 1992. Late Proterozoic low-latitude global glaciation: the Snowball Earth. In: J.W. Schopf and C. Klein (eds.), The Proterozoic Biosphere: a multidisciplinary study. Cambridge University Press, pp. 51-52.

Koeberl, C., 1998. Identification of meteoritic components in impactites. In: M.M. Grady, , R. Hutchision, G.J.H. McCalland D.A. Rothery (eds.), Meteorites: Flux with Time and Impact Effects. Geological Society London Special Publication, 140, pp. 133-152.

Koeberl, C., 2014. The geochemistry and cosmochemistry of impacts. In: H.D. Holland and K.K. Turekian (eds.), Treatise on Geochemistry, Second Edition, vol. 2 (Planets, Asteroids, Comets and The Solar System). Elsevier, Oxford, pp. 73-118.

Koeberl, C., Claeys, P., Hecht, L. and McDonald, I., 2012. Geochemistry of impactites. Elements, 8, 37-42.

Koeberl, C., Ivanov, B.A. and Goodman, B.A., 2007a. Impact triggering of the Snowball Earth deglaciation? Bridging the Gap II: Effect of Target Properties on the Impact Cratering Process, Abstracts of the conference held September 22-26, 2007 in Saint-Hubert, Canada. Lunar and Planetary Institute Contribution No. 1360, pp. 62-63.

Koeberl, C., Ivanov, B.A., and Goodman J., 2007b. Impact-induced deglaciation of the Snowball Earth? EOS Trans. American Geophysical Union 88(52), Fall Meet. Suppl., Abstract U22A-08.

Kring, D.A., 2003. Environmental consequences of impact cratering events as a function of ambient conditions on Earth. Astrobiology, 3, 133-152.

Mader, D. and Koeberl, C., 2009. Using Instrumental Neutron Activation Analysis for geochemical analyses of terrestrial impact structures: Current analytical procedures at the University of Vienna Geochemistry Activation Analysis Laboratory. Applied Radiation and Isotopes, 67, 2100-2103.

Martin, H., 1965. Beobachtungen zum Problem der jung-präkambrischen glazialen Ablagerungen in Südwestafrika (Observations concerning the problem of the late Precambrian glacial deposits in South West Africa). Geologische Rundschau, 54, 115-127.

Montanari, A. and Koeberl, C., 2000. Impact stratigraphy: the Italian record. Lectures Notes in Earth Sciences, 93, Heidelberg, Springer Verlag. 364 pp.

Peucker-Ehrenbrink, B. and Hoffman, P.F., 2006. Sedimentary PGE anomalies at Snowball Earth terminations. (abstract). Geochimica et Cosmochimica Acta, 70, A488.

Rudnick, R.L. and Gao, S., 2003. Composition of the Continental Crust. In: H.D. Holland, and K.K. Turekian (eds.), Treatise on Geochemistry, Volume 3. Elsevier, pp. 1-64.

Stöffler D. and Langenhorst F., 1994. Shock metamorphism of quartz in nature and experiment: I. Basic observations and theory. Meteoritics, 29, 155-181.

Waters, C., Peucker-Ehrenbrink, B. and Hoffman, P.F., 2009. Platinum group element and Re-Os isotope systematics of Cryogenian glacial terminations. (abstract) American Geophysical Union, Fall Meeting 2009, abstract #U13A-0047.

Waters, C., Peucker-Ehrenbrink, B. and Hoffman, P.F., 2010. Platinum group element and Re-Os isotope systematics of Cryogenian glacial terminations. (abstract) Geochimica et Cosmochimica Acta, 74, A1117.

Williams, G.E., 2000. Geological constraints on the Precambrian history of Earth's rotation and the Moon's orbit. Reviews of Geophysics, 38/1, 37-59.

Received: 5 December 2013
Accepted: 20 November 2014

Ildikó GYOLLAI[1)2)3)], Dieter MADER[1)], Márta POLGÁRI[3)*)], Friedrich POPP[4)] & Christian KOEBERL[1)5)]

[1)] Department of Lithospheric Research, University of Vienna, Althanstrasse 14, 1090 Vienna, Austria;

[2)] Cosmic Materials Research Group, Eötvös Loránd University of Budapest (ELTE), Pázmány Péter sétány 1/A, 1117 Budapest, Hungary;

[3)] Research Center for Astronomy and Geosciences, Geobiomineralization and Astrobiological Research Group, Institute for Geology and Geochemistry, Hungarian Academy of Sciences, Budaörsi út 45, 1112 Budapest, Hungary;

[4)] Department of Geodynamics and Sedimentology, University of Vienna, Althanstrasse 14, 1090 Vienna, Austria;

[5)] Natural History Museum, Vienna, Burgring 7, 1010 Vienna, Austria;

[*)] Corresponding author, rodokrozit@gmail.com